

Acetone laser induced fluorescence for low pressure/low temperature flow visualization

R. A. Bryant, J. M. Donbar, J. F. Driscoll

471

Abstract Acetone fluorescence provides a useful way to visualize the fluid mixing process within supersonic wind tunnels, some of which operate in the low temperature (240–300 K) and low pressure range (0.1–1 atm). Measurements are presented to quantify the dependence of the acetone laser induced fluorescence (LIF) signal on temperature and pressure in this range. The temperature and pressure sensitivity of the acetone LIF signal resulted in less than an 8% variation over the experimental conditions for a laser excitation wavelength of 266 nm. Condensation of the acetone vapor was identified as a potential problem for this diagnostic technique. Methods to prevent and check for condensation are discussed.

1 Introduction

In both reacting and non-reacting mixing studies, one way to quantify the amount of mixing is to seed either the fuel or oxidizer with a suitable marker fluid such as acetone vapor and then visualize the marker fluid using laser induced fluorescence (LIF). LIF is especially attractive for use in high speed flows because it provides excellent temporal and spatial resolution. For example, the mixing due to parallel jet injection from a strut into a supersonic airstream was visualized in the supersonic mixing facility at Wright-Patterson Air Force Base by Glawe et al. (1994). In their experiment, a sonic jet of helium was seeded with acetone and mixing occurred in the low temperature range from 200–300 K and low pressure range from 0.1–1 atm. To quantify the rate of mixing from the LIF images in

supersonic wind tunnels it is necessary to know how the fluorescence signal depends on temperature and pressure.

While numerous studies of acetone LIF have been conducted in the past, there has not been any calibration information reported for temperatures below 300 K and only recently has information been made available that spans the pressure range 0.1–1 atm. Additional work also is needed because the acetone LIF calibration may be sensitive to the excitation wavelength and the laser intensity. It is agreed that the dominant deexcitation path for excited acetone molecules is intersystem crossing (ISC) from the singlet state to a triplet state which occurs with an efficiency of almost unity (Breuer and Lee 1971; Halpern and Ware 1971; Hansen and Lee 1975). Heicklen (1959) found that the acetone fluorescence efficiency was independent of gas pressure, which suggested that collisional quenching is a negligible deexcitation path from the first excited singlet state. Tait and Greenhalgh (1990) reported a linear temperature dependence of acetone LIF per molecule over the range 300–700 K using 308 nm excitation. They suggest that the fluorescence originates from both the singlet and triplet states. The triplet state, being subject to quenching, is therefore the source of the temperature dependence. The recent results of Thurber et al. (1998) provide a comprehensive calibration of the acetone LIF per molecule for the temperature range of 300–975 K and various excitation wavelengths (248–320 nm). Their work suggests that a shift to longer wavelengths of the absorption spectrum combined with changing rates of singlet to triplet ISC is responsible for the temperature dependence observed. Grossmann et al. (1996) report the pressure and temperature behavior of acetone LIF per molecule for excitations at 248, 277 and 312 nm. Their results show an initial increase of the relative acetone LIF signal with increasing gas pressure; the gas pressure sensitivity however decreases at longer excitation wavelengths. Their temperature behavior reported is similar to that observed by Thurber et al. (1998). Wolff et al. (1993) investigated the fluorescence of an acetone/air mixture in a heated static cell for presumably a 248 nm excitation. Their results of single shot laser measurements show approximately $\pm 4\%$ variation of the acetone LIF over the pressure range of 0.05–18 atm and approximately $\pm 14\%$ variation over the temperature range of 300–675 K. Yuen et al. investigated the pressure dependence of acetone LIF for a 266 nm excitation in four different buffer gases. The fluorescence quantum efficiency increased by approximately 45% with increasing gas pressure from 0.6–5 atm for each buffer gas.

Received: 5 October 1998/Accepted: 10 April 1999

R. A. Bryant¹, J. M. Donbar², J. F. Driscoll
Department of Aerospace Engineering
University of Michigan
Ann Arbor, MI 48109-2118

Present addresses:

¹National Institute of Standards and Technology, Building and Fire Research Laboratory, Gaithersburg, MD 20899-8653

²Aero Propulsion and Power Directorate, Wright-Patterson Air Force Base, Dayton, OH 45433

Correspondence to: R. A. Bryant

This work was supported by the Aero Propulsion and Power Directorate, Wright-Patterson AFB; Dr. Abdi Nejad served as contract monitor.

Ossler and Alden measured the effective lifetimes of the first excited state of acetone when excited at 266 nm. Their results show that the effective lifetime, which is directly proportional to the fluorescence quantum efficiency, increases with increasing pressure and decreases with increasing temperature.

The present work extends the previous database for a single laser excitation wavelength of 266 nm and for a single buffer gas, air. It quantifies the temperature and pressure dependence of acetone LIF signals in the range 240–300 K and 0.1–1 atm, which are typical operating conditions of supersonic wind tunnels. The lowest temperature considered in the previously mentioned studies was 300 K. A static cell was designed to accommodate both low temperature and pressure. The problems associated with acetone condensation in the low temperature range are discussed along with the subsequent solutions. LIF measurements that check for signal linearity and photodecomposition of the acetone molecules were conducted in order to ensure proper interpretation of the results.

2 Experimental procedure

2.1 Apparatus

A static gas chamber was used which was cooled to 230 K while providing gas pressures ranging from 0.02–1 atm. The stainless steel cylindrical chamber, shown in Fig. 1, had internal dimensions of 15.24 cm \times 20.32 cm (diameter \times length). Two fused quartz windows allowed for the entry and exit of the ultraviolet laser beam. A third quartz window allowed for the collection of the LIF signal. The chamber was cooled by liquid nitrogen which flowed through copper tubing coiled about its exterior.

A mixture of acetone vapor and dry air was prepared in a second chamber with a similar volume to the test chamber. The mixture was transferred to the test chamber which had been evacuated and cooled. Dry air was added to the test chamber until the desired mole fraction of ac-

etone vapor was achieved. Fluorescence measurements were collected at 10 K intervals as the mixture passively warmed to room temperature (295 K). The gas temperature was monitored by thermocouples (type J) at three locations along the chamber centerline and the chamber wall temperature was monitored by two surface thermocouples (type J). Gas pressure was monitored by a digital pressure transducer (OMEGA PX136-015A-V).

A frequency quadrupled Quanta-Ray GCR 250 Nd:YAG laser delivered a 266 nm laser beam to excite the acetone molecules. The beam was approximately 6 mm in diameter with a repetition rate of 10 Hz and pulse width of 10 ns. Due to the homogeneity of the gas mixture, the beam was unfocused since spatial resolution was not a concern. The pulse-to-pulse laser energy was monitored by a UV sensitive fast photodiode (Thorlabs DET2-SI), while the average laser energy was monitored by a disc calorimeter (Scientech 38-1UV5). Typical average energy flux of the beam was 88 mJ/cm². A RCA 4526 photomultiplier tube (PMT) was oriented perpendicular to the laser beam axis to collect the fluorescence emission. A bi-convex glass lens, with $f/1.0$, focused the collection volume with 1:1 imaging onto the PMT slit opening. The glass lens also served as a filter for the elastically scattered UV light. A background signal was recorded by irradiating the chamber of dry air with the 266 nm laser beam before the acetone vapor was added. The background signal, which accounts for scattered LIF from the entry and exit quartz windows and any possible fluorescence from the glass lens due to the elastically scattered light, was subtracted from each measured LIF signal. A signal to noise ratio of 60 was achieved for the averaged signal over 300 laser pulses. The fluorescence spectrum was collected with a GCA/McPherson Model 216.5 monochromator which employed a RCA 931A PMT. Output signals from the PMT and photodiode were collected by a Stanford Research Systems Model SR250 gated integrator. The resulting data files were stored on a Micron 486 DX computer for later analysis.

2.2 Techniques to avoid acetone condensation at low temperatures

Investigation of acetone fluorescence at low temperatures presented some challenging problems such as nonuniform cooling, icing of optical access windows and condensation of the acetone vapor. The access ports for pressure, temperature, laser beam, etc. made it difficult to employ a uniform wrap of copper tubing around the chamber. The tubing wrap was divided into three sections with limited control of the liquid nitrogen flow through each section by shut off valves. Control of the liquid nitrogen flow rate combined with passive heating of the chamber, reduced the differences in the measured gas temperature among the three centerline thermocouples to less than 6 K in the lower limit of the temperature range. Condensation on the exterior of the optical access windows was eliminated by providing a constant jet of room temperature air across the windows. Interior condensation of water was eliminated by using a dry air mixture in the chamber.

Early in the investigation problems were incurred with the acetone vapor condensing on the chamber walls. The

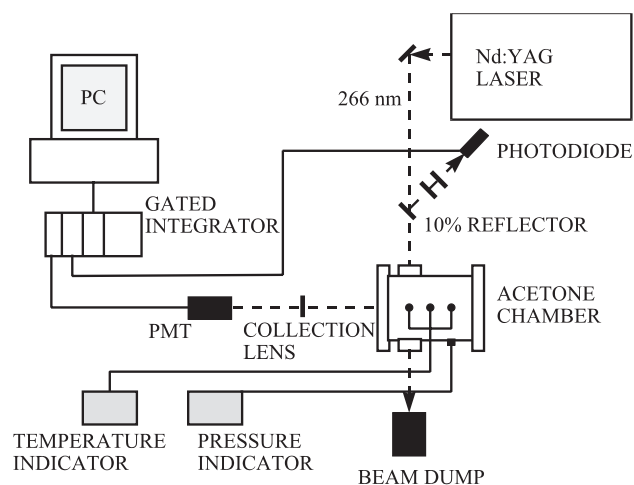


Fig. 1. Experimental arrangement for low temperature, low pressure acetone LIF studies

gas mixture and the chamber were cooled simultaneously and the LIF signal was reduced to less than 10% of the reference signal at room temperature. A check for condensation was performed by evacuating the gas mixture from the chamber after it had been cooled and then measuring the LIF signal after the evacuated chamber had warmed to room temperature. The resulting LIF signal was 90% of the reference signal at room temperature and atmospheric pressure, therefore confirming that much of the acetone vapor had condensed to liquid form on the chamber walls. Surface thermocouples were employed and wall cold spots were found to exist when the chamber was cooled rapidly. Temperatures at these cold spots could be as low as 140 K, 70 K below the gas temperature on centerline. Condensation would occur at these cold spots if the mole fraction of acetone vapor exceeded the saturation limit for the local temperature.

The saturation mole fraction of acetone with respect to temperature, shown in Fig. 2, is an empirical relation derived by Ambrose et al. (1974). The figure shows that for a typical mole fraction of acetone, $X_{\text{act}} = 9.0 \times 10^{-5}$, condensation will be a problem if at any location within the chamber the local temperature falls below 185 K. Condensation of the acetone vapor was avoided by not introducing the acetone/dry air mixture into the cell until the liquid nitrogen flow had been halted and the walls had been allowed to warm to 200 K. The typical acetone mole fraction that was introduced into the chamber was maintained at approximately five times less than the mole fraction at the saturation limit for 200 K, so condensation was no longer a problem.

2.3

Theoretical relation for the fluorescence signal

The results reported in this section are compared to the theoretical relation for the acetone fluorescence signal that is derived by Hanson et al. (1990) and is given by:

$$S_F = C\eta \frac{\Omega}{4\pi} \left(\frac{E_L}{(\pi d^2/4)\Delta t h\nu} \right) (n_a V) \sigma_a \Phi_F \quad (1)$$

The signal, S_F , is a voltage representing the photons per second received at the photo detector; the constant C rep-

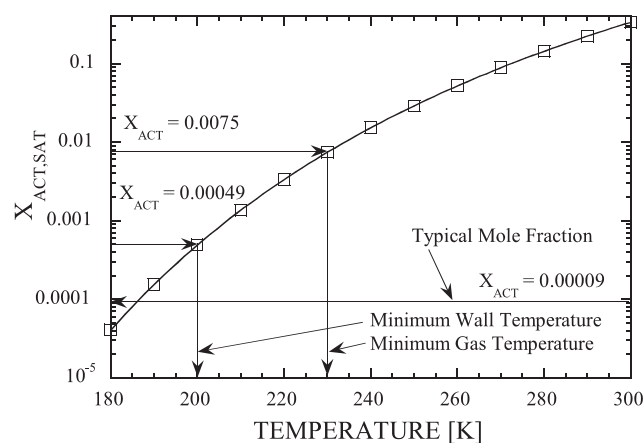


Fig. 2. Acetone saturation curve (Ambrose et al. 1974)

resents the gain of the detector and the proper conversion factors. The collection optics efficiency and solid angle are η and Ω , respectively. E_L is the laser energy per pulse; d is the beam diameter; Δt is the pulse duration, and ν is the excitation frequency. The acetone number density is n_a and V is the collection volume. The absorption cross section is σ_a (cm^2) and the fluorescence quantum yield is Φ_F .

It is useful to note that the signal S_F in Eq. (1) is proportional to the fraction of photons traveling along the laser beam that collide with the target acetone molecules. This fraction of photons that collide is proportional to $(N_a \sigma_a)/(\pi d^2/4)$, which is the ratio of the total target area ($N_a \sigma_a$) to the beam cross sectional area; $N_a = n_a V$ is the number of target molecules. The number of photons/sec traveling along the beam is $E_L/(\Delta t h\nu)$.

The fluorescence yield in Eq. (1) is shown to be:

$$\Phi_F = \left(1 + \frac{k_{\text{ISC}}}{k_F} + \frac{k_Q}{k_F} + \frac{k_{\text{IC}}}{k_F} + \frac{k_D}{k_F} \right)^{-1} \quad (2)$$

where k_F is the rate of fluorescence (s^{-1}) from the first excited singlet state; k_{ISC} is the rate of excited singlet to triplet state intersystem crossing (s^{-1}); k_{IC} is the rate of internal conversion from the excited singlet to the ground state and k_D is the rate of photodecomposition from the excited singlet state (Breuer and Lee 1971). The rate of quenching from the excited singlet state is $k_Q = \sum_i n_i \bar{c} \sigma_{Qi}$, where n_i is the number density of collisional species i ; \bar{c} is the mean thermal speed and σ_{Qi} is the collisional quenching cross section (cm^2) of species i (Schofield and Steinberg 1981). Since ISC is the dominate energy relaxation process from the singlet state, only the second term has significant contribution to Eq. (2).

3

Results – Effect of acetone number density on the LIF signal

Equation (1) is valid only if the laser beam energy flux is sufficiently low so that saturation is not a problem. The range of energy flux resulting in a linear relation between the LIF signal and laser energy flux is shown in Fig. 3. The maximum measured flux was approximately 350 mJ/cm^2 . The acetone number density was varied by evacuating known percentages of an initial concentration from the test chamber. Figure 4 shows the recorded LIF signals referenced to the signal collected from the initial mixture and confirms the direct proportionality of the acetone number density to the LIF signal for linear LIF and constant temperature and pressure.

Degradation of the acetone molecules due to photodecomposition was a major concern since the sample was contained in a static chamber. Figure 5 illustrates how a given sample of acetone vapor degraded as it was exposed to increasing numbers of laser pulses. The rate at which the sample degraded increased as the laser flux was increased. In order to maintain a constant acetone number density over the duration of an experiment, constraints on the laser energy and the total number of laser shots were applied. An operating laser energy flux of 88 mJ/cm^2 was chosen for all conditions and no sample was subjected to more than 3000 laser pulses; therefore limiting the loss of acetone molecules to photodecomposition to less than 2%.

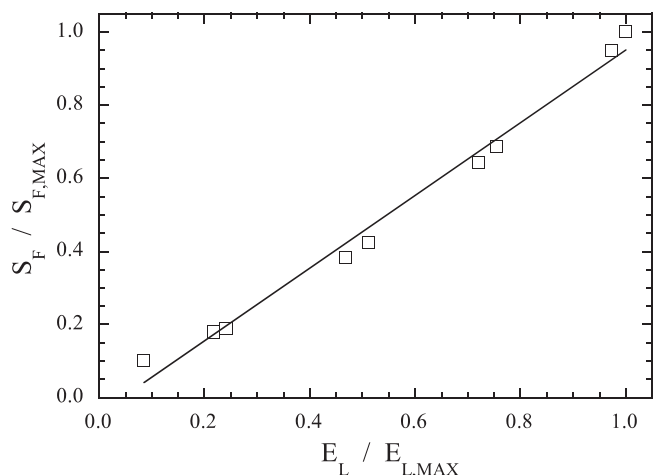


Fig. 3. Acetone LIF signal, S_F , as a function of measured laser energy per unit pulse, E_L . Maximum laser energy was 100 mJ/pulse, corresponding to an energy per unit area of 353 mJ/cm²

Acetone emission has a long-lived component, phosphorescence, which must be distinguished from the short-lived component, fluorescence. Temporal discrimination was applied by the gated integrator which acquired the emission signal within a 40 ns interval centered about the 10 ns laser pulse. Therefore only fluorescence was collected and not the longer lived phosphorescence. Previous studies concluded that the unwanted acetone phosphorescence is quenched by trace amounts of oxygen (Damon and Daniels 1933; Heicklen 1959; Hunt and Noyes 1948). The present mixtures were greater than 99% air.

4 Results – Effects of pressure and temperature on the LIF

The theoretical relation for the LIF signal is given by Eq. (1). If it is normalized by the reference signal measured at a selected reference pressure p_0 and reference temperature T_0 it follows that:

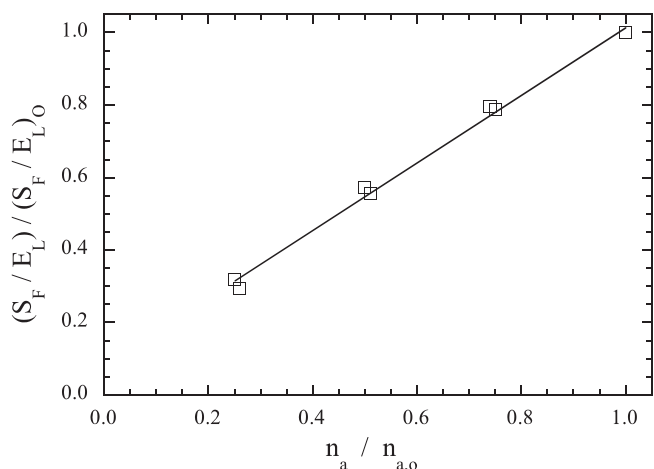


Fig. 4. Normalized acetone LIF signal, S_F/E_L , as a function of acetone number density, n_a . Laser energy per unit area was 88 mJ/cm²; energy/pulse was 25 mJ/pulse; $n_{a,0} = 2.21 \times 10^{15}$ cm⁻³, corresponding to a mole fraction of 9.20×10^{-5} at STP

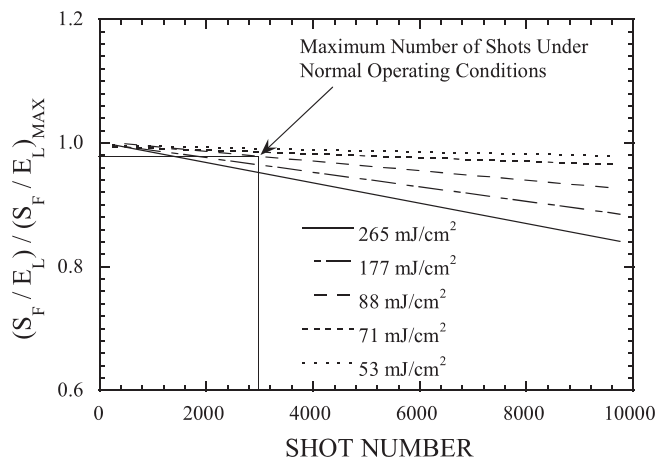


Fig. 5. Acetone degradation rate due to dissociation of the acetone molecule by the laser pulse. Operating conditions were chosen as shown: maximum laser pulses/sample = 3000, maximum laser energy/unit area = 88 mJ/cm². Therefore the effects of acetone degradation were less than 2%

$$\frac{(S_F/E_L)}{(S_F/E_L)_0} = \frac{n_a}{n_{a,0}} F(T, p, \lambda) \quad (3)$$

where $F = (\sigma_a \Phi_F) / (\sigma_{a,0} \Phi_{F,0})$, which were defined previously.

Thurber et al. (1998) demonstrated that σ_a and Φ_F are sensitive to temperatures exceeding 300 K, therefore the goal of the present study is to perform a calibration of Eq. (3) at temperatures and pressures below STP conditions for a fixed wavelength of 266 nm. Since the terms in Eq. (1) with possible temperature and pressure sensitivity were not individually investigated, their combined behavior are represented in the function, F . The acetone number density was held constant ($n_a = n_{a,0}$) and the pressure was varied in the following manner. An initial mass of acetone vapor was introduced into the evacuated chamber and then the pressure was increased by adding dry air to the chamber at 295 K. As the air was added, the acetone number density remained constant because the number of moles of acetone and the chamber volume remained constant.

Figure 6 shows that the fluorescence signal varies by $\pm 5\%$ over the pressure range of 0.1–1 atm. Each measurement point corresponds to the mean over 300 successive laser pulses. Four separate experimental runs were conducted each consisting of 10 separate measurements. The results are consistent with the results of Yuen et al. (1997), who report a $\sim 5\%$ increase in the acetone fluorescence quantum efficiency from 0.6–1 atm, in air and for a 266 nm excitation. Grossmann et al. (1996) report a $\sim 15\%$ increase of the acetone LIF intensity from 0–1 atm, in 383 K synthetic air and for a 248 nm excitation. They also state that the pressure sensitivity decreases with increasing excitation wavelength. Ossler and Alden (1997) show a 10–20% increase in the effective fluorescence lifetime of acetone as the air pressure increases from 0–1 atm (at 323 K) for a 266 nm excitation. The associated uncertainty of their measurements suggest that the trend of the

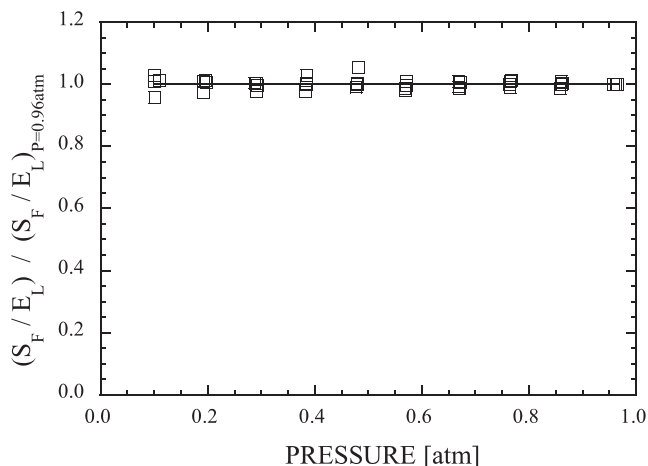


Fig. 6. Effect of gas pressure on acetone LIF signal. Temperature = 295 K, $n_a = 2.21 \times 10^{15} \text{ cm}^{-3}$

pressure sensitivity be considered for comparison to the present results.

The effect of gas temperature was determined by measuring the acetone LIF signal as the cooled gas mixture was warmed from 240 K to room temperature. Figure 7 shows that the LIF signal was decreased by less than 8% at the gas temperature of 240 K. The data is the result of 3 separate experiments and each point represents the mean over 300 successive laser pulses. The results extend the measurements of Thurber et al. (1998) who reported less than a 10% decrease of the fluorescence emitted per molecule over the range of 300–400 K for a 266 nm excitation.

Acetone fluorescence emission spectrums, shown in Fig. 8, were measured at temperatures of 230 K and 296 K. Each spectrum is normalized by its maximum value and corrected for the detection system transmission and responsivity. The spectrums are almost identical, indicating that the emission relaxation process of the excited molecules is consistent over this temperature range. Each emission spectrum is the result of approximately 3000 laser shots. The small change in the gas composition due

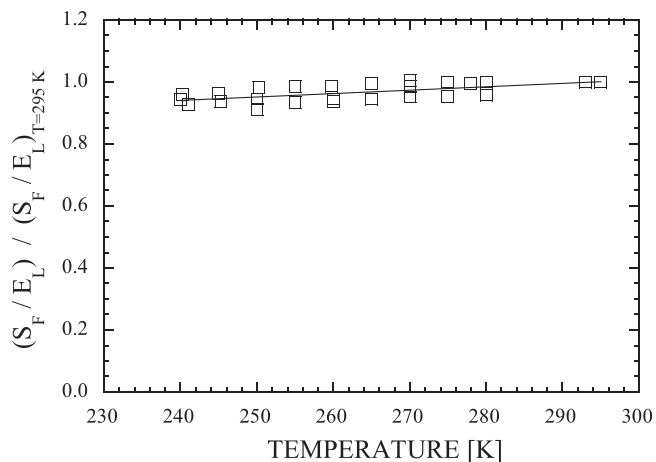


Fig. 7. Effect of gas temperature on acetone LIF signal. $n_a = 2.21 \times 10^{15} \text{ cm}^{-3}$

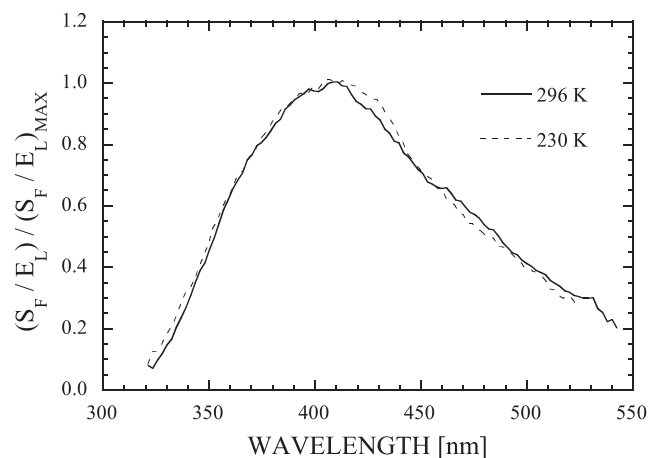


Fig. 8. Spectrum of acetone LIF signal at 230 K and 296 K

to photodecomposition demonstrates no apparent effect on the emission spectrum.

5 Method to measure gas mixture fraction (f)

When two gases, A and B, undergo turbulent mixing in a nonreacting flow, it is useful to measure the mass fraction of gas A. This mass fraction is denoted as the mixture fraction, f . The mass fraction of the other gas, B, thus is $1-f$. The mixture fraction f is related to the mole fraction of gas A by:

$$f = \left[\left(1 - \frac{M_B}{M_A} \right) + \frac{M_B}{M_A} \frac{1}{X_A} \right]^{-1} \quad (4)$$

where M_A and M_B are the known molecular weights of gas A (including the acetone vapor) and gas B. Assuming that the reference condition is a location where only the seeded gas A exists ($X_{A,0} = 1$, $X_{B,0} = 0$) it follows that:

$$\frac{n_a}{n_{a,0}} = \frac{n_A}{n_{A,0}} = X_A \frac{p \cdot T_0}{p_0 \cdot T} \quad (5)$$

Combining Eqs. (3) and (5) and solving for X_A yields:

$$X_A = \frac{p_0 (S_F/E_L) (T/T_0)}{p (S_F/E_L)_0 F(T, p, \lambda)} \quad (6)$$

Finally, by combining Eqs. (4) and (6), the mixture fraction f can be measured from the resulting equation:

$$f = \left[\left(1 - \frac{M_B}{M_A} \right) + \frac{M_B (S_F/E_L)_0 p F(T, p, \lambda)}{M_A (S_F/E_L) p_0 (T/T_0)} \right]^{-1} \quad (7)$$

Thus it is possible to infer the mixture fraction f from the measured acetone LIF signal, S_F , but the local pressure and temperature also must be measured using other diagnostics. As expected, Eq. (7) has a simple form if the molecular weights of gases A and B happen to be equal ($M_B = M_A$) and if, in addition, the gas pressure and temperature are constant at all locations; in this case Eq. (7) becomes:

$$f = \frac{(S_F/E_L)}{(S_F/E_L)_0} \quad (8)$$

Conclusions

The pressure and temperature dependence of the acetone LIF signal for a 266 nm excitation was determined at low temperature and low pressure conditions which are characteristic of certain supersonic wind tunnels. A 5% variation of the relative acetone LIF signal intensity was observed as the gas pressure increased from 0.1–1 atm. Similar studies have reported a slight increase in the acetone LIF as the gas pressure was increased over this region. Therefore the present finding that pressure, over the range of 0.1–1 atm, does not significantly affect the acetone LIF signal, implies that gas pressure does not need to be measured independently in order to deduce the fuel number density from the LIF data. The acetone LIF signal also was only a weak function of gas temperature, increasing by only 6% as the gas temperature was increased from 240–295 K. The results extend the current database of acetone LIF temperature behavior and demonstrate that the need for a separate temperature measurement in this region is not necessary in order to properly interpret the acetone LIF signal. Therefore, within a level of uncertainty, it is possible to directly infer the acetone number density from the acetone LIF signal. However, to infer the gas mixture fraction, measurements of temperature and pressure are necessary. The significant problem of cooling acetone vapor without causing condensation was overcome by issuing the vapor into an already cooled gas cell whose walls had warmed to desired values and by setting maximum limits on the acetone mole fractions. Dry air was chosen as the primary gas because it is used in practical mixing applications and the oxygen present quenches any unwanted phosphorescence.

References

- Ambrose D; Sprake CHS; Townsend R (1974) Thermodynamic properties of organic oxygen compounds - XXXIII. The vapour pressure of acetone. *J Chem Thermodynamics* 6: 693–700
- Breuer GM; Lee EKC (1971) Fluorescence decay times of cyclic ketones, acetone, and butanal in the gas phase. *J Phys Chem* 75: 989–990
- Damon GH; Daniels F (1933) The photolysis of gaseous acetone and the influence of water. *J Am Chem Soc* 55: 2363–2375
- Glawe DD; Donbar JM; Nejad AS; Sekar B; Chen TH; Samimy M; Driscoll JF (1994) Parallel fuel injection from the base of an extended strut into supersonic flow. AIAA paper 94-0711, 32nd Aerospace Sciences Meeting, Reno, NV
- Grossmann F; Monkhouse PB; Ridder M; Sick V; Wolfrum J (1996) Temperature and pressure dependencies of the laser-induced fluorescence of gas-phase acetone and 3-pentanone. *Appl Phys B* 62: 249–253
- Halpern AM; Ware WR (1971) Excited singlet state radiative and nonradiative transition probabilities for acetone, acetone-d₆, and hexafluoroacetone in the gas phase, in solution, and in the neat liquid. *J Chem Phys* 54: 1271–1276
- Hansen DA; Lee EKC (1975) Radiative and nonradiative transitions in the first excited singlet state of symmetrical methyl-substituted acetones. *J Chem Phys* 62: 183–189
- Hanson RK; Seitzman JM; Paul PH (1990) Planar laser-fluorescence imaging of combustion gases. *Appl Phys B* 50: 441–454
- Heicklen J (1959) The fluorescence and phosphorescence of biacetyl vapor and acetone vapor. *J Am Chem Soc* 81: 3863–3866
- Hunt RE; Noyes WA (1948) Photochemical studies. XXXIX. A further study of the fluorescence of acetone. *J Am Chem Soc* 70: 467–476
- Ossler F; Alden M (1997) Measurements of picosecond laser induced fluorescence from gas phase 3-pentanone and acetone: Implications to combustion diagnostics. *Appl Phys B* 64: 493–502
- Schofield K; Steinberg M (1981) Quantitative atomic and molecular laser fluorescence in the study of detailed combustion processes. *Opt Engr* 20: 501–510
- Tait NP; Greenhalgh DA (1992) 2D laser induced fluorescence imaging of parent fuel fraction in nonpremixed combustion. Twenty-Fourth Symposium (International) on Combustion/ The Combustion Institute 1621–1628
- Thurber MC; Grisch F; Kirby BJ; Votsmeier M; Hanson RK (1998) Measurements and modeling of acetone laser-induced fluorescence with implications for temperature-imaging diagnostics. *Appl Opt* 37: 4963–4978
- Wolff D; Schluter H; Beushausen V; Andresen P (1993) Quantitative determination of fuel air mixture distributions in an internal combustion engine using PLIF of acetone. *Ber Bunsenges Phys Chem* 97: 1738–1741
- Yuen LS; Peters JE; Lucht RP (1997) Pressure dependence of laser-induced fluorescence from acetone. *Appl Opt* 36: 3271–3277